

## PAPER

## Recyclable nanoscale copper(I) catalysts in ionic liquid media for selective decarboxylative C–C bond cleavage

Cite this: *Catal. Sci. Technol.*, 2013, **3**, 992

Michael T. Keßler, Christian Gedig, Sebastian Sahler, Patricia Wand, Silas Robke and Martin H. G. Prechtl\*

Received 7th November 2012,  
Accepted 20th December 2012

DOI: 10.1039/c2cy20760e

[www.rsc.org/catalysis](http://www.rsc.org/catalysis)

Here we report the synthesis and application of finely divided Cu<sub>2</sub>O nanoparticles (Cu<sub>2</sub>O-NPs) in the range from 5.5 nm to 8.0 nm in phosphonium ionic liquids as the first recyclable and effective catalytic system for smooth, ligand- and additive-free protodecarboxylation of 2-nitrobenzoic acid as a model substrate and further derivatives. The reactions run with low catalyst loadings and result in quantitative yield in ten consecutive recycling experiments. In addition this system is highly selective towards electron-poor 2-nitrobenzoic acids.

Catalysts are crucial mediators for most reactions in synthesis. They are used for bond-breaking and bond-making reactions in the sustainable production of bulk- and fine-chemicals.<sup>1–3</sup> In recent years modern nanocatalysis has attracted much interest in this field of scientific research as a useful and efficient tool for functionalisation and defunctionalisation reactions.<sup>4,5</sup> Carboxyl groups belong to the most common functionalities in organic molecules and catalytic decarboxylation reactions are therefore extremely useful and environmentally benign tools to eliminate surplus carboxylate groups in organic compounds. Furthermore decarboxylative carbon–carbon cross coupling reactions are initiated by a decarboxylative step of a carboxylate salt, which represents a cheap substitute for expensive organometallic (e.g. organo-boron, organo-tin, organo-zinc) reagents.<sup>6</sup>

Nowadays metal nanoparticles, such as ruthenium,<sup>7–15</sup> platinum,<sup>16</sup> iridium,<sup>17–19</sup> palladium,<sup>5,20–31</sup> cobalt,<sup>32</sup> and iron,<sup>33</sup> have great potential for application<sup>34</sup> in homogeneous and heterogeneous catalysis, including hydrogenation,<sup>7</sup> hydrogenolysis,<sup>35</sup> Fischer–Tropsch reactions<sup>32,36</sup> and cross-coupling reactions.<sup>4,5,21,23</sup> Copper<sup>37</sup> and especially copper(I)oxide<sup>38</sup> nanoparticles combine the high catalytic activity of precious metals with easy availability and low cost. One drawback of neat metal and metal oxide nanoparticles is their poor recyclability and leaching effects leading to decreasing yields.<sup>39</sup> To overcome this problem, usually expensive nitrogen or phosphorus containing ligands, surfactants or polymers are used to protect the nanoparticle surface from agglomeration, aggregation and leaching.<sup>7,21</sup> Ionic liquids (ILs) are promising reagents for

surface protection, stabilising agents as well as green, non-hazardous solvents.<sup>40</sup> Ionic liquids exhibit a negligible vapour pressure, tuneable solubilisation properties for several organic and inorganic compounds and are (electro-) chemically inert. Additionally an ionic liquid phase containing the metal or metal oxide catalyst can be recycled several times without significant drop of yield.<sup>23,40–42</sup> Nitrogen containing ionic liquids, such as imidazolium, pyridinium or pyrrolidinium ILs, with various counter anions are commonly used in nanocatalysis recycling experiments.<sup>38,40,43</sup> There are some reports about application of copper and copper oxide nanoparticles in ionic liquids, however most of them are related to electrochemistry and microelectronics and only very few report about application as catalysts in the wide field of organic synthesis.<sup>37,38,40,44–54</sup> The first report about colloidal copper catalysts for the coupling of aryl halides and activated olefins was reported by Heck and Nolley in 1972.<sup>54</sup> More recently, it has been shown that nanoscale copper catalysts are released from copper bronze in ionic liquid media and these particles were active in the Heck reaction.<sup>45</sup> Further copper nanoparticle IL systems were active in well-known reactions like the Stille,<sup>46</sup> Sonogashira,<sup>44</sup> and Buchwald–Hartwig coupling.<sup>47</sup> Moreover, copper nanocatalysts in IL support the coupling of aryl halides with ammonia yielding anilines,<sup>55</sup> diaryl ethers (or thioethers) are obtained by coupling phenols with aryl halides,<sup>40,50,53</sup> and unexpected coupling of olefins with THF was observed.<sup>49</sup> Unsurprisingly, copper nanocatalysts are also active in the homocoupling of alkynes, known as Ullmann coupling.<sup>48,52</sup>

A challenging reaction for the evaluation of nanoscale catalysts is the protodecarboxylation reaction.<sup>56,57</sup> Notably, this reaction has not been evaluated yet for nanoscale catalysts in ionic liquids. Usually the model system for copper catalysts

University of Cologne, Department of Chemistry, Institute of Inorganic Chemistry, Greinstraße 6, 50939 Cologne, Germany. E-mail: martin.prechtl@uni-koeln.de; Web: <http://catalysis.uni-koeln.de>; Fax: +49 221 4701788

is the Ullmann reaction.<sup>5,48,52</sup> The protodecarboxylation reaction is a very smart method to defunctionalise an electron deficient aromatic ring carrying a carboxylic acid as a potential leaving group in the presence of a Cu(I) catalyst. While highly activated carboxylic acids (e.g. perfluorinated benzoic acids) readily decarboxylate without any catalyst,<sup>58</sup> the removal of the carboxylate groups from simple aromatic acids is much more complicated and often requires harsh reaction conditions, an inadequate use of copper or even more expensive silver salts as well as large amounts of additives.<sup>59</sup> In the present work we show that nanoscale copper(I)oxide (Cu<sub>2</sub>O-NPs) embedded in ionic liquids is an active and recyclable catalyst for this reaction.

## Synthesis of Cu<sub>2</sub>O nanoparticles

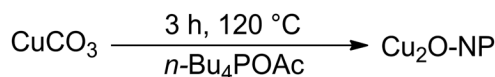
The copper(I)oxide nanoparticles presented here were synthesised *via* thermal decomposition of basic CuCO<sub>3</sub> in different ionic liquid media. In this system no additional reducing agent, such as hydrazine or hydrogen, is necessary for the reduction of Cu(II) to Cu(I). We assume that the structural nature and polarity of the ionic liquid plays a beneficial role in the reductive formation of Cu<sub>2</sub>O nanoparticles. In previous works it has been shown that Pd nanoparticles are obtained by thermal decomposition of Pd(OAc)<sub>2</sub> in IL.<sup>60</sup> Furthermore, studies about the formation of ruthenium and nickel nanoparticles by decomposition of organometallic precursors in ionic liquids showed that (I) the anion plays an important role and (II) the IL itself is capable of inducing the decomposition by reaction with a complex.<sup>9</sup> In these cases minor amounts of IL suffered from decomposition and only traces of volatile compounds were detected in the gaseous phase, indicating decomposition of the IL.

The nanoparticle synthesis in 3-butyl-1,2-dimethylimidazolium bis(trifluoromethyl-sulfonyl)imide (bmmim NTf<sub>2</sub>) led to bulk material of Cu<sub>2</sub>O (Table 1, entry 1). Other imidazolium based ionic liquids (3-butyl-1-methylimidazolium bis(trifluoromethyl-sulfonyl)imide (bmim-NTf<sub>2</sub>) or pyridinium based ionic liquids (butylpyridinium bis(trifluoromethyl-sulfonyl)imide (bpy NTf<sub>2</sub>)) were not capable of decomposing the copper salt even at elevated temperatures (Table 1, entries 2 and 3). The use of

**Table 1** Various ionic liquids for Cu<sub>2</sub>O nanoparticle synthesis

Entry	Cu	IL	T (°C)	NP	Size <sup>a</sup> (nm)	Cu(I) <sub>surface</sub> (%)
1	CuCO <sub>3</sub>	bmmim NTf <sub>2</sub>	120	Bulk	Bulk	
2	CuCO <sub>3</sub>	bmim-NTf <sub>2</sub>	120	n.d.	n.d.	
3	CuCO <sub>3</sub>	bpy NTf <sub>2</sub>	120	n.d.	n.d.	
4	CuCO <sub>3</sub>	C <sub>3</sub> CNmim NTf <sub>2</sub>	120	n.d.	n.d.	
5	<b>CuCO<sub>3</sub></b>	<b><i>n</i>-Bu<sub>4</sub>POAc</b>	<b>120</b>	<b>Cu<sub>2</sub>O</b>	<b>5.5</b> (± 1.2)	<b>35</b>
6	CuCO <sub>3</sub>	( <i>n</i> -Bu <sub>4</sub> P) <sub>2</sub> SO <sub>4</sub>	120	n.d.	n.d.	
7	<b>CuCO<sub>3</sub></b>	<b>(<i>n</i>-Bu<sub>4</sub>P)<sub>2</sub>SO<sub>4</sub></b>	<b>160</b>	<b>Cu<sub>2</sub>O</b>	<b>8.0</b> (± 2.7)	<b>26</b>
8	Cu(NO <sub>3</sub> ) <sub>2</sub>	<i>n</i> -Bu <sub>4</sub> POAc	160	n.d.	n.d.	
9	Cu(OAc) <sub>2</sub>	<i>n</i> -Bu <sub>4</sub> POAc	160	n.d.	Bulk	
10	CuI	<i>n</i> -Bu <sub>4</sub> POAc	160	n.d.	n.d.	
11	CuF <sub>2</sub>	<i>n</i> -Bu <sub>4</sub> POAc	160	n.d.	n.d.	

Reaction conditions: Cu = 1 mmol Cu salt, 1 g IL, 3 h; n.d. = no decomposition. <sup>a</sup> Particle size was determined by TEM.



**Scheme 1** Cu<sub>2</sub>O nanoparticle synthesis in *n*-Bu<sub>4</sub>POAc.

copper(II)acetate did not improve the quality of particles either – no stable dispersion was observed, but bulk material was formed which indicates very fast decomposition. We tried a large variety of other simple copper salts, such as copper nitrate, but there was no decomposition into Cu<sub>2</sub>O detected. We switched to alkyl-phosphonium-ILs as a low melting and more polar reaction medium. Tetrabutylphosphonium acetate (*n*-Bu<sub>4</sub>POAc) and tetrabutylphosphonium sulphate ((*n*-Bu<sub>4</sub>P)<sub>2</sub>SO<sub>4</sub>) seemed adequate because of their lower melting point and polarity in contrast to nitrogen containing ILs (Scheme 1).

We were able to synthesise Cu<sub>2</sub>O nanoparticles with small size and narrow size-distribution by simple thermal decomposition at 120 °C for 3 h as undoubtedly confirmed by TEM and XRD. To explain the exact reaction pathway of the formation of Cu(I), we analysed the dispersion of the Cu<sub>2</sub>O-NPs in (*n*-Bu<sub>4</sub>POAc) IL by <sup>1</sup>H-NMR and <sup>31</sup>P-NMR, as well as by means of gaseous phase analysis using online-mass spectrometry.

After the completed nanoparticle synthesis, the <sup>31</sup>P- as well as the <sup>1</sup>H-NMR spectra showed no decomposition of the phosphonium cation at 120 °C, but the signals of the acetate protons completely vanished (Fig. 1, δ = 1.83 ppm). This indicates that Hofmann elimination does not play a relevant role in the reduction of Cu(II) to Cu(I), during the thermal treatment in *n*-Bu<sub>4</sub>POAc at 120 °C, and it confirms that the acetate is capable to act as a reducing agent of the copper salt. Similar observations are known for other metal acetates.<sup>60</sup> During Hofmann elimination one would obtain trialkyl phosphine which could then subsequently result in trialkyl phosphine oxide and Cu(I). However, the phosphonium cation remains mainly intact, whereas large amounts of CO<sub>2</sub> are formed due to decomposition of the acetate ions which can be detected by mass spectrometry. The analysis of the gaseous phase by mass spectrometry showed only minor decomposition products (butene fragments; *m/z* = 56 and 55) of the degradation of the phosphonium cation in contrast to the extrusion of CO<sub>2</sub> (Fig. 2). This means, the IL itself acts as a reducing and surface-protecting agent as well as the solvent.

We detected large amounts of carbon dioxide (*m/z* = 44) in the gaseous phase (Fig. 2), indicating that acetate ions are

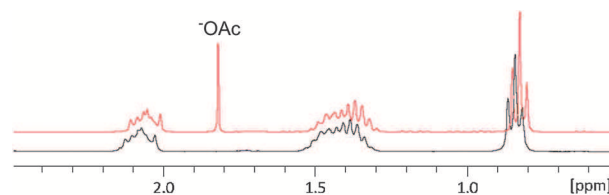


**Fig. 1** <sup>1</sup>H-NMR spectra of *n*-Bu<sub>4</sub>POAc before (upper spectrum) and after (lower spectrum) the decomposition of CuCO<sub>3</sub>. The acetate signal (δ = 1.83 ppm) disappeared completely.

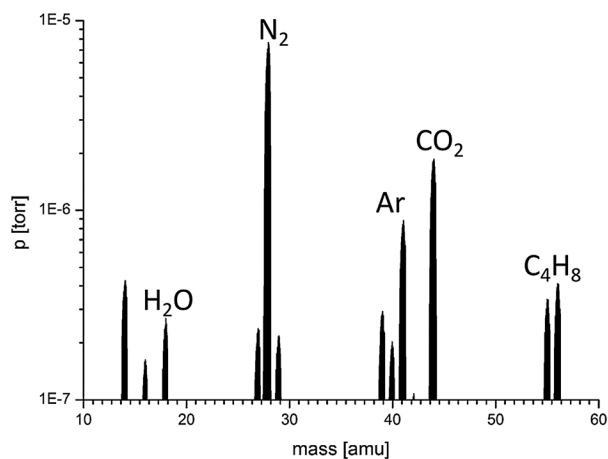


**Fig. 2** Online gas-phase mass-spectrogram recorded after the decomposition of  $\text{CuCO}_3$  in  $n\text{-Bu}_4\text{POAc}$  at  $120^\circ\text{C}$ .

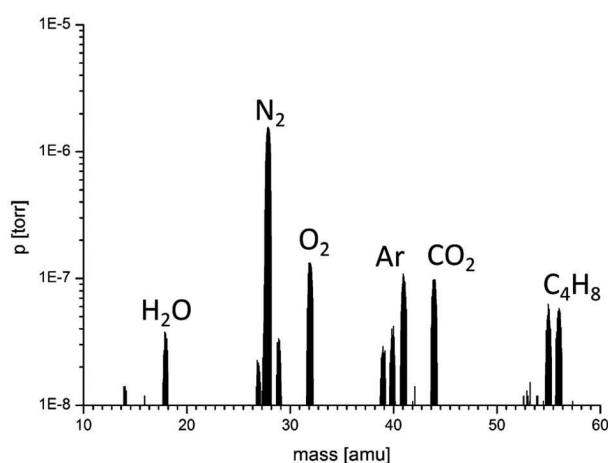


**Fig. 3** Online gas-phase mass-spectrogram recorded after the decomposition of  $\text{CuCO}_3$  in  $(n\text{-Bu}_4\text{P})_2\text{SO}_4$  at  $160^\circ\text{C}$ .

decomposed and act as a reducing agent for the metal(II) species, where the IL cation plays a minor role for the reduction of the metal(II) species, but influences the stabilisation of NPs.<sup>60</sup> Further detected components were dinitrogen ( $m/z = 28/14$ ), water ( $m/z = 18$ ) and other components of air.

For the decomposition in  $(n\text{-Bu}_4\text{P})_2\text{SO}_4$ , where no acetate ions are present, the reduction only takes place at elevated temperatures ( $160^\circ\text{C}$ ) and Hofmann elimination products are detectable in a further gas-phase mass-spectrogram (Fig. 3) and in the  $^{31}\text{P}$ -NMR spectrum a new peak appears (Fig. 4,  $\delta = 57.5$  ppm).

A significant amount of butene fragments ( $m/z = 56$  and  $55$ ) is detectable in the gas-phase mass-spectrogram during the decomposition of  $\text{CuCO}_3$  in  $(n\text{-Bu}_4\text{P})_2\text{SO}_4$  at  $160^\circ\text{C}$ . Other signals correspond to air compounds like, oxygen, nitrogen and water. Furthermore a new phosphorus species (tributyl phosphine oxide) is detectable in the  $^{31}\text{P}$ -NMR spectrum ( $57.5$  ppm),<sup>61</sup> taken from the reaction mixture right after completion of the nanoparticle synthesis.

Due to the extremely low vapour pressure of the ionic liquids, the  $\text{Cu}_2\text{O}$  nanoparticles could be characterised directly

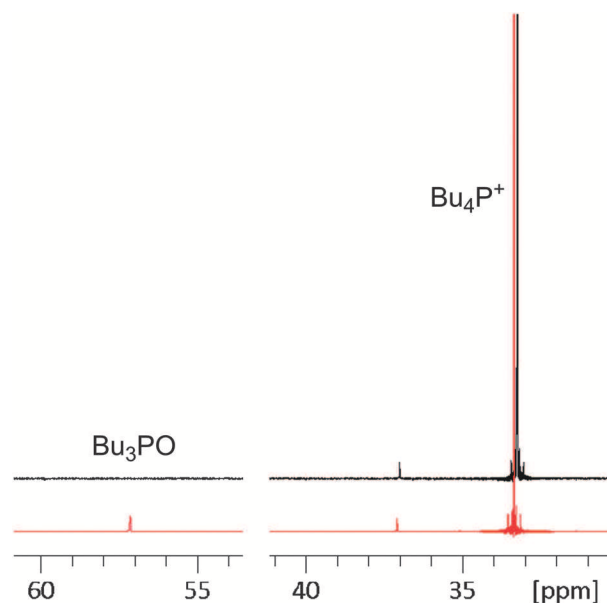


**Fig. 4**  $^{31}\text{P}$ -NMR spectra of  $(n\text{-Bu}_4\text{P})_2\text{SO}_4$  before (upper spectrum) and after (lower spectrum) the decomposition of  $\text{CuCO}_3$  at  $160^\circ\text{C}$ . The signal at  $57.5$  ppm corresponds to tributylphosphine oxide.<sup>61</sup>

in the IL medium using TEM techniques and additionally by XRD. TEM pictures of  $\text{Cu}_2\text{O}$  nanoparticles both in  $n\text{-Bu}_4\text{POAc}$  and in  $(n\text{-Bu}_4\text{P})_2\text{SO}_4$  are shown in Fig. 5 and 6. The average

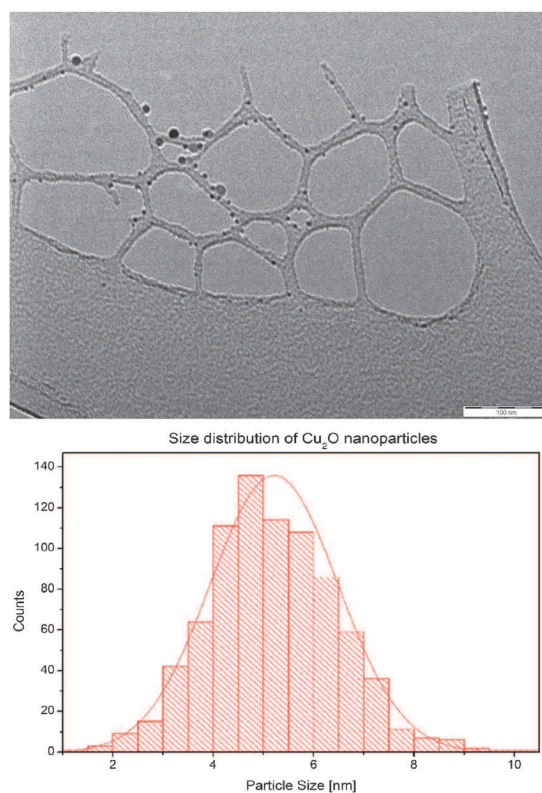


**Fig. 5** TEM picture (top) of  $\text{Cu}_2\text{O}$  nanoparticles synthesised in  $n\text{-Bu}_4\text{POAc}$  and size distribution (bottom) – the average diameter is  $5.5$  nm ( $\pm 1.2$  nm). The scale bar of the TEM image is  $100$  nm.

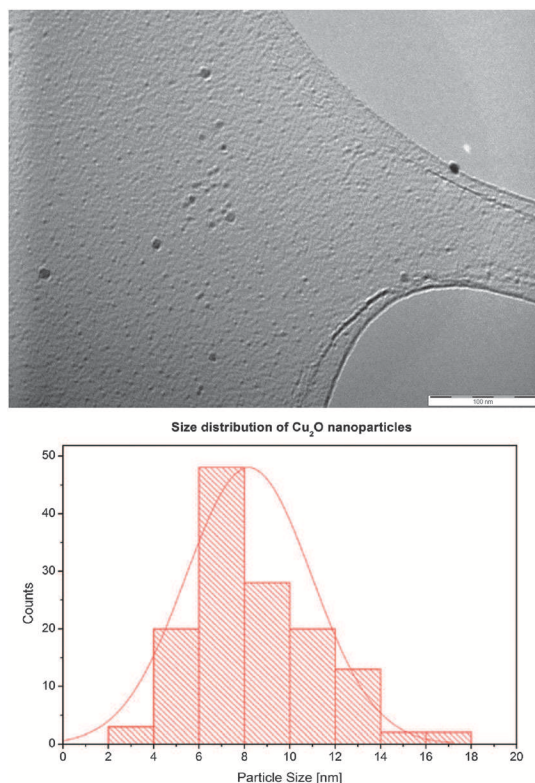


**Fig. 6** TEM picture (top) of  $\text{Cu}_2\text{O}$  nanoparticles synthesised in  $(n\text{-Bu}_4\text{P})_2\text{SO}_4$  and size distribution (bottom) – the average diameter is 8.0 nm ( $\pm 2.7$  nm). The scale bar of the TEM image is 100 nm.

diameter of the monodispersed and uniformly shaped  $\text{Cu}_2\text{O}$  nanoparticles is about 5.5 nm ( $\pm 1.2$  nm) in  $n\text{-Bu}_4\text{POAc}$  and 8.0 nm ( $\pm 2.7$  nm) in  $(n\text{-Bu}_4\text{P})_2\text{SO}_4$ , respectively. The different sizes of the NP arise from two different reaction mechanisms and reaction temperatures in the decompositions. In  $(n\text{-Bu})_4\text{POAc}$  at 120 °C the acetate ion is the reductant whereas in  $((n\text{-Bu})_4\text{P})_2\text{SO}_4$  a higher temperature is necessary (160 °C) and Hofmann elimination of the tetrabutylphosphonium cations leads to tributylphosphine which readily reduces  $\text{Cu(II)}$  to give  $\text{Cu(I)}$  and tributylphosphine oxide. The particles are finely separated and show a homogeneous spherical shape. The XRD pattern clearly shows pure  $\text{Cu}_2\text{O}$  without any impurities

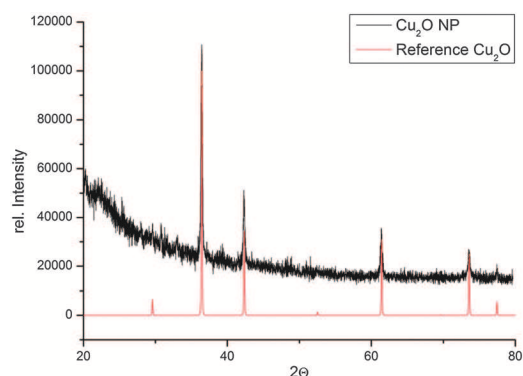


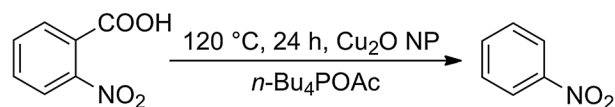
**Fig. 7** XRD pattern of  $\text{Cu}_2\text{O}$  (cubic  $\text{Cu}_2\text{O}$ ) nanoparticles synthesised in tetrabutylphosphonium ionic liquid  $n\text{-Bu}_4\text{POAc}$ .

of other copper species (Fig. 7). The signals at small angles originate from the preparation foil for the XRD samples. According to the Scherrer equation the nanocrystallite size corresponds to 24 nm, which is larger than the particle size determined by TEM analysis, which might be due to aggregation during preparation of the XRD-powder sample (see experimental section), however, it confirms the formation of  $\text{Cu}_2\text{O}$ -nanoparticles. Moreover, the size of nanoparticles in powder XRD patterns is often overestimated in case of a broader particle size distribution, *vice versa* for a very narrow size distribution determined by TEM the nanocrystallite size determined by XRD fits well.<sup>62,63</sup> In the present case of the larger particles the vast majority of copper(I)oxide is in the inner shells of the nanoparticles. This results in large reflexes in the XRD patterns which overlay reflexes of smaller particles. The estimated diameter by the Scherrer equation can therefore be considered as an upper size limit of the nanoparticles in the NP-IL dispersion. Regarding the evaluation of the nanoscale  $\text{Cu}_2\text{O}$  for their application in catalysis, the surface to volume ratio of the particles must be considered. Although we cannot exclude that some partial aggregations and topology changes might occur,<sup>64</sup> merely copper ions on the surface are capable of acting as a catalyst.

For the determination of the percentage of copper ions in  $\text{Cu}_2\text{O}$  exposed to the surface, we calculated the volume of a spherical particle of  $\text{Cu}_2\text{O}$  in  $n\text{-Bu}_4\text{POAc}$  with a diameter of 5.5 nm. The volume is about 87.1 nm<sup>3</sup> containing approx. 4477  $\text{Cu(I)}$  ions. Applying the *magic number* methodology,<sup>65–67</sup> as the established tool for the general evaluation of cluster formation and surface to volume ratio, the particle contains approximately 1563  $\text{Cu(I)}$  ions exposed to the surface (taking into account the stoichiometry and composition of the elemental cell of  $\text{Cu}_2\text{O}$ ). This means that  $\sim 35\%$  of the  $\text{Cu(I)}$  are surface ions and potentially active in a heterogeneous catalysed reaction. For the  $\text{Cu}_2\text{O}$ -NPs in  $(n\text{-Bu}_4\text{P})_2\text{SO}_4$  with a mean diameter of 8.0 nm about  $\sim 26\%$  of the  $\text{Cu(I)}$  are surface ions. Interestingly, the obtained nanoparticles form dispersions in other solvents such as acetone, isopropanol or even water, which make them highly interesting for synthetic application in nanocatalytic reactions and multiphase reactions.

## Protodecarboxylation reaction

For the evaluation of the catalytic properties of the  $\text{Cu}_2\text{O}$  nanoparticles, we chose the protodecarboxylation reaction. This reaction has been tested previously only with molecular copper complexes, copper salts, but not with nanoscale catalysts and none of the previous catalyst systems was suitable for recycling<sup>56,57</sup> (Scheme 2).



**Scheme 2** Protodecarboxylation of 2-nitrobenzoic acid **1** with  $\text{Cu}_2\text{O}$  nanoparticles in  $n\text{-Bu}_4\text{POAc}$ .

**Table 2** Variation of the reaction conditions and ionic liquid media for the protodecarboxylation of 2-nitrobenzoic acid **1**

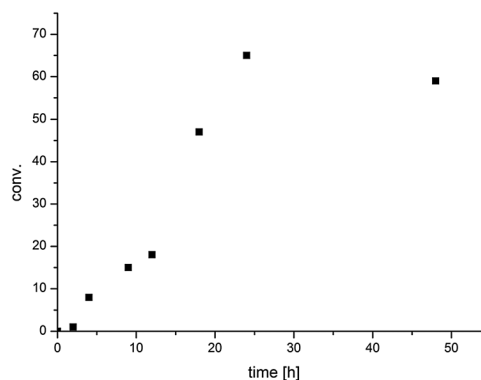
Entry	Cu source	IL	Additives	<i>T</i> (°C)	Conv. <sup>f</sup> (%)
1	Cu <sub>2</sub> O-NPs <sup>a</sup>	<i>n</i> -Bu <sub>4</sub> P·OAc	—	80	<1
2	Cu <sub>2</sub> O-NPs <sup>a</sup>	<i>n</i> -Bu <sub>4</sub> P·OAc	—	120	61
3	Cu <sub>2</sub> O-NPs <sup>a</sup>	<i>n</i> -Bu <sub>4</sub> P·OAc	KF, K <sub>2</sub> CO <sub>3</sub>	120	59
4	Cu <sub>2</sub> O-NPs <sup>a</sup>	<i>n</i> -Bu <sub>4</sub> P·OAc	KF	120	58
5	Cu <sub>2</sub> O-NPs <sup>a</sup>	<i>n</i> -Bu <sub>4</sub> P·OAc	K <sub>2</sub> CO <sub>3</sub>	120	55
6	Cu <sub>2</sub> O-NPs <sup>b</sup>	<b><i>n</i>-Bu<sub>4</sub>P·OAc</b>	—	120	100
7	Cu <sub>2</sub> O-NPs <sup>c</sup>	( <i>n</i> -Bu <sub>4</sub> P) <sub>2</sub> SO <sub>4</sub>	—	160	51
8	CuCO <sub>3</sub> <sup>d</sup>	bmim·Ms	—	120	39
9	Cu(OAc) <sub>2</sub> <sup>d</sup>	bmim·Ms	—	120	24
10	Cu(NO <sub>3</sub> ) <sub>2</sub> <sup>d</sup>	bmim·Ms	—	160	39
11	CuCO <sub>3</sub> <sup>d</sup>	C3CNmim OAc	—	120	23
12	Cu <sub>2</sub> O <sup>e</sup>	<i>n</i> -Bu <sub>4</sub> P·OAc	—	120	20

Reaction conditions: <sup>a</sup> 1 mmol 2-nitrobenzoic acid **1**, Cu<sub>2</sub>O-NPs (35 mol%<sub>surface</sub>) in 1 g IL. <sup>b</sup> With Cu<sub>2</sub>O-NPs (105 mol%<sub>surface</sub>) <sup>c</sup> Cu<sub>2</sub>O-NPs (17.5 mol%<sub>surface</sub>) in 1 g IL. <sup>d</sup> 1 mmol 2-nitrobenzoic acid **1**, 1 mmol Cu-source in 1 g IL. <sup>e</sup> Commercial copper(I)oxide. Reaction time: 24 h. <sup>f</sup> Conversions were determined by <sup>1</sup>H NMR and hexamethyldisilane as the internal standard.

The nanoscale copper catalysts have been prepared as described above using CuCO<sub>3</sub>. Additionally Cu(OAc)<sub>2</sub> and Cu(NO<sub>3</sub>)<sub>2</sub> have been tested in ionic liquid media for the protodecarboxylation under different reaction conditions for the decarboxylation of 2-nitrobenzoic acid **1** (Table 2). Then the benzoic acid derivative and optional additives as well as water were added to the reaction medium. Quantitative yield could be obtained with Cu<sub>2</sub>O nanoparticles derived from copper carbonate (3 mmol) in *n*-Bu<sub>4</sub>P·OAc (Table 2, entry 6). Considering that ~35% of the Cu(I) are surface ions, roughly 1.05 mmol (105 mol%<sub>surface</sub>) of the Cu(I) in the particle is potentially active for promoting the C–C bond cleavage reaction in benzoic acid **1**. Upon lowering the copper concentration to 1 mmol, 35 mol%<sub>surface</sub> of the Cu(I) are exposed to the surface, remarkably still 61% of the benzoic acid **1** is catalytically decarboxylated at 120 °C (entry 2). A catalyst loading of 17.5 mol%<sub>surface</sub> Cu<sub>2</sub>O nanoparticles in (*n*-Bu<sub>4</sub>P)<sub>2</sub>SO<sub>4</sub> IL showed a conversion in the same range (51%) at 160 °C (entry 7). Taking into account the larger particle size of the Cu<sub>2</sub>O-NPs in (*n*-Bu<sub>4</sub>P)<sub>2</sub>SO<sub>4</sub> (8.0 nm) the activity is comparable to those in *n*-Bu<sub>4</sub>P·OAc. Interestingly the initially used additives like KF and K<sub>2</sub>CO<sub>3</sub> were not necessary for the reaction nor did they improve yields. The reaction shows remarkable temperature sensitivity. At temperatures below 100 °C no product could be obtained (entry 1). The optimal temperature is between 120 °C and 160 °C depending on the IL and the used copper salt.

The best conversions using Cu<sub>2</sub>O-NPs (35 mol%<sub>surface</sub>) could be obtained after 24 h as shown in Fig. 8. After an initiation period of about two hours, the yield increases almost linearly reaching a high value of 65% after 24 h and then stagnates. Even a reaction time of about 48 h does not lead to an enhanced conversion.

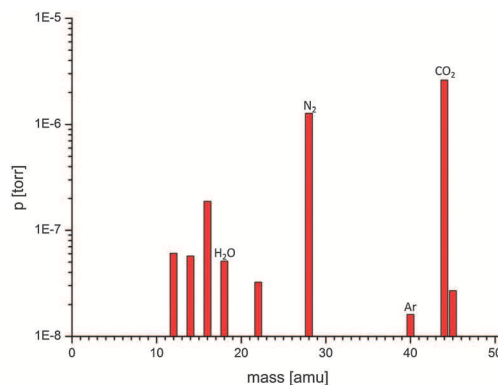
3-Butyl-1-methylimidazolium bis(trifluoromethyl-sulfonyl)-imide (bmim·NTf<sub>2</sub>) is a relatively nonpolar ionic liquid, which does not dissolve inorganic salts sufficiently and is not miscible with water, has been proven to be unsuitable for the decarboxylation reaction. A simple and halide-free polar ionic liquid is

**Fig. 8** Conversion of 2-nitrobenzoic acid **1** into nitrobenzene **2** in *n*-Bu<sub>4</sub>P·OAc at 120 °C depending on the reaction time.

3-butyl-1-methyl imidazolium methylsulfonate (bmim·Ms; entries 8–10). Although bmim·Ms is a nitrogen containing IL with a high melting point, it is readily soluble in water and forms a viscous liquid. The conversions of the protodecarboxylation in bmim·Ms were <40%, but significantly lower than in *n*-Bu<sub>4</sub>P·OAc (entry 2).

Interestingly, in bmim·Ms it is even possible to use copper salts like Cu(OAc)<sub>2</sub> or Cu(NO<sub>3</sub>)<sub>2</sub> to promote the decarboxylation of 2-nitrobenzoic acid **1**. The activation energy of the decarboxylation depends on the copper-source (Cu<sub>2</sub>O-NP, Cu(NO<sub>3</sub>)<sub>2</sub>, Cu(OAc)<sub>2</sub>,...) and on the polarity of the solvating medium ((*n*-Bu<sub>4</sub>P·OAc, (*n*-Bu<sub>4</sub>P)<sub>2</sub>SO<sub>4</sub>, bmim·Ms,...). The formation and stabilisation of two transition states during the decarboxylation step are crucial for the reaction temperature, which has already been calculated using DFT methods by Su and co-workers.<sup>68</sup> All polar ionic liquids used here form homogeneous suspensions, and the organic products can be easily separated by extraction with nonpolar organic solvents. The relatively high viscosity of the catalytic phase simplifies the extraction and separation step with *e.g.* Et<sub>2</sub>O or *n*-pentane, therefore the organic product can be easily isolated and the catalytically active IL-phase is recyclable for further batch experiments.

The gaseous products have been analysed by mass-spectrometry. The mass spectrum (Fig. 9) shows clearly that no further

**Fig. 9** Mass spectrum of the gas phase in a typical protodecarboxylation reaction measured at 1.75 bar.

side reaction took place and that CO<sub>2</sub> is extruded in high amounts.

About 61% of the analysed gas probe corresponds to carbon dioxide ( $m/z = 44$ ), 30% dinitrogen and 4% oxygen as well as minor amounts of nitrogen and water. The probe was taken directly out of the autoclave system *via* a mass flow controller.

## Recycling experiments

As previously described, the phosphonium ionic liquids used here are superior concerning nanoparticle protection, due to long term stabilisation of the nanoparticle dispersions. Additionally, the ILs exhibit a polarity, which makes them interesting for recycling experiments. The product nitrobenzene **2** can be separated by extraction with a nonpolar organic solvent without leaching of the nanoparticles or of the ionic liquid itself. Interestingly the residual phase containing the Cu<sub>2</sub>O nanoparticles can be recycled several times (up to ten times, see below), by simple reloading with carboxylic acid as a substrate. In the following diagram the recycling experiments with the corresponding yields are shown (Fig. 10).

The best results concerning long-term stability of the catalyst, recyclability and conversion have been obtained in *n*-Bu<sub>4</sub>POAc with an amount of 105 mol%<sub>surface</sub> of Cu<sub>2</sub>O-NPs, quantitative conversion has been obtained in almost all runs giving a total TON of ~88 accumulated over the ten runs (Fig. 10; black scales). After ten runs the catalyst loading can be considered as 10.5 mol%<sub>surface</sub>. Catalyst loadings of 70 mol%<sub>surface</sub> Cu<sub>2</sub>O-NPs (7.0 mol%<sub>surface</sub> after ten runs) showed after the initial first run quantitative conversion in the next three runs, then the conversions decreased significantly after each run (Fig. 10; dark grey scale). Upon lowering the catalyst loading to 35 mol%<sub>surface</sub> (3.5 mol%<sub>surface</sub> in ten runs) the yields increased after the first run drastically and reached a remarkable high yield of about 96% (Fig. 10; dashed grey scale). Even after five cycles there was a considerable amount of nitrobenzene **2** detectable and up to eight reactions in one batch could be carried out.

The recycling experiments with CuCO<sub>3</sub> in bmim·Ms showed low conversions (<40%) over four runs and then no further activity was observed (light grey scales). Although silver salts are

known to be superior decarboxylation catalysts,<sup>59,69</sup> Ag<sub>2</sub>CO<sub>3</sub> in bmim·Ms only resulted in conversions <40% in four runs (Fig. 10; grey scale bars; left). Obviously the ionic liquid itself plays a crucial role in both the nanoscale decarboxylation reaction and in the nanoparticle synthesis.

## Substrate scope of benzoic acid derivatives

To prove the versatility of the nanocatalyst system we performed the decarboxylation reaction on different benzoic acid derivatives. The reaction could be performed with moderate to good conversions with 2-nitrobenzoic acid derivatives (Table 3 entries 1–10). Conversions of about 65% to 40% could be reached with halide substituents of a 2-nitrobenzoic acid derivative in *para*-position (entries 5 and 6). Other electron-withdrawing groups in *para*-position, like a nitro- or a trifluoromethyl-group, seem to be beneficial, too (entries 1 and 2). Only low conversions could be reached with substituents in *meta*-position (entries 7–9) except methyl-groups (entries 4 and 10). Interestingly no conversion of other benzoic acid derivatives could be observed (entries 11–22) – even with highly electron-deficient benzoic acids, like 2-chloro-4-nitrobenzoic acid (entry 13) and 2-chloro-4-fluorobenzoic acid (entry 17). In fact, the nitro group in *ortho*-position seems to be crucial for the nanoparticle catalysed decarboxylation of the benzoic acid derivatives – maybe due to a coordination of the nitro-group to the surface of a nanoparticle. In contrast, a single nitro group in *para*-position did not lead to an increase in conversion (entry 12).

## Chemo-selectivity in mixtures of benzoic acids

One very important issue is the selectivity of decarboxylation reactions towards different benzoic acid derivatives. Usually copper catalysed protodecarboxylation reactions can be easily conducted with benzoic acids containing an electron deficient aromatic ring-system – no matter which kind of substituents they bear.<sup>56</sup> Therefore, we tried to decarboxylate selectively the model substrate in a reaction mixture with different benzoic acids. This nanocatalytic approach is the first that can selectively decarboxylate 2-nitrobenzoic acid **1** in the presence of other benzoic acids with comparable electron poor aromatic rings with considerable yields. Even 4-nitro-2-chloro benzoic acid **4** is not affected under the reaction parameters given here (Table 4, entry 2). In all cases the selectivity for decarboxylation was 100% towards **1** (Table 4). Interestingly, the yield of the decarboxylation product, nitrobenzene **2**, varied between 23% and 78% depending on the presence of the second benzoic acid. The lowest conversion of 2-nitrobenzoic acid **1** into nitrobenzene **2** was obtained in the presence of 4-chloro-2-fluoro benzoic acid **3** (23%; Table 4, entry 1), and the highest conversion (78%) was possible in the presence of 2-sulfonic benzoic acid **5**. The influence of the second benzoic acid regarding the different conversions during the decarboxylation of 2-nitrobenzoic acid **1** is still unclear.

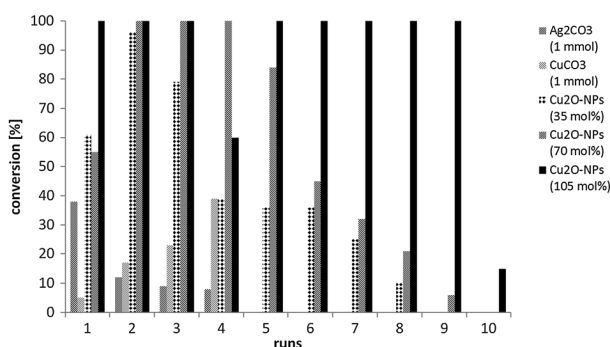
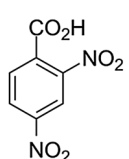
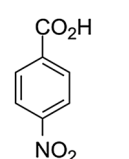
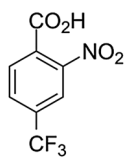
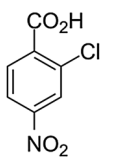
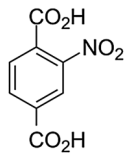
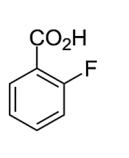
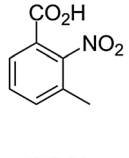
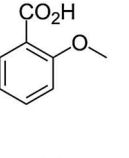
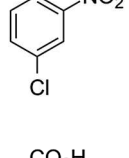
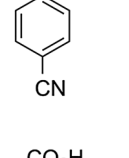
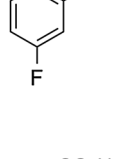
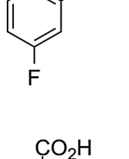
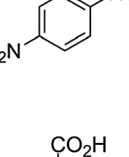
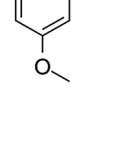
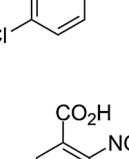
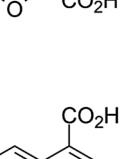
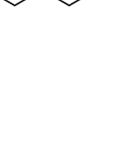
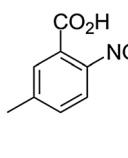
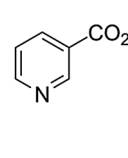
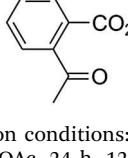
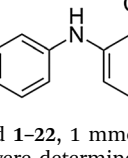


Fig. 10 Recycling experiments of the decarboxylation of 2-nitrobenzoic acid **1** in IL media.

**Table 3** Substrate screening for protodecarboxylation reactions of different benzoic acids in *n*-Bu<sub>4</sub>POAc with Cu<sub>2</sub>O nanoparticles

Entry	Acid	Conv. <sup>a</sup> (%)	Entry	Acid	Conv. <sup>a</sup> (%)
1		24	12		0
2		32	13		0
3		10	14		0
4		30	15		0
5		65	16		0
6		40	17		0
7		10	18		0
8		21	19		0
9		15	20		0

**Table 3 (continued)**

Entry	Acid	Conv. <sup>a</sup> (%)	Entry	Acid	Conv. <sup>a</sup> (%)
10		26	21		0
11		0	22		0

Reaction conditions: 1 mmol benzoic acid 1–22, 1 mmol Cu<sub>2</sub>O in 1 g *n*-Bu<sub>4</sub>POAc, 24 h, 120 °C. <sup>a</sup> Conversions were determined by <sup>1</sup>H NMR and hexamethyldisilane as the internal standard.

**Table 4** Chemo-selectivity of the nanoscale protodecarboxylation in the presence of a selection of different benzoic acid derivatives

Entry	Acid A <sup>a</sup>	Acid B <sup>b</sup>	Conv. (%) A : B	Selectivity (%) A : B
1	1	12	57 : 0	100 : 0
2	1	13	39 : 0	100 : 0
3	1	15	50 : 0	100 : 0
4	1	16	48 : 0	100 : 0
5	1	17	23 : 0	100 : 0
6	1	18	47 : 0	100 : 0
7	1	23	78 : 0	100 : 0
8	1	24	62 : 0	100 : 0

Reaction conditions: <sup>a</sup> Acid A: 1 mmol 2-nitrobenzoic acid 1, Acid B: 1 mmol benzoic acid (4-nitrobenzoic acid 12, 4-nitro-2-chloro benzoic acid 13, 2-methoxybenzoic acid 15, 4-cyanobenzoic acid 16, 2-chloro-4-fluoro benzoic acid 17, 4-methoxybenzoic acid 18, 2-sulfonic benzoic acid 23, 4-aminobenzoic acid 24), Cu<sub>2</sub>O-NPs (35 mol%<sub>surface</sub>) in 1 g IL, reaction time: 24 h. <sup>b</sup> Conversions were determined by <sup>1</sup>H NMR and hexamethyldisilane as the internal standard.

## Experimental

### General

*n*-Bu<sub>4</sub>POH in 40 wt% aqueous solution, basic CuCO<sub>3</sub>, CuF<sub>2</sub> and all benzoic acids (1–24) were obtained from ABCR<sup>®</sup> Chemicals, CuI and methylimidazole were purchased from Sigma Aldrich<sup>®</sup>, methane sulfonyl chloride was purchased from Fluka<sup>®</sup>. Cu(NO<sub>3</sub>)<sub>2</sub> and Cu(OAc)<sub>2</sub> were used from chemicals stock of the institute. All chemicals were used without further purification and all reactions were conducted without inert conditions.

<sup>1</sup>H-NMR and <sup>31</sup>P-NMR spectra were recorded on a Bruker<sup>®</sup> AVANCE II 300 spectrometer at 298 K (300.1 MHz, external standard tetramethylsilane (TMS)). The obtained Cu<sub>2</sub>O nanoparticles were analysed by powder X-ray diffractometry (STOE<sup>®</sup>-STADI MP, Cu-K<sub>α</sub> irradiation, λ = 1.540598 Å) and by a TEM Phillips<sup>®</sup> EM 420, 120 kV. Mass spectra were recorded on a HIDDEN<sup>®</sup> HPR-20QIC equipped with a Bronkhorst<sup>®</sup> EL-FLOW Select mass flow meter/controller. Experiments for gas phase analysis at elevated pressure were performed in a stainless steel autoclave purchased from Carl-Roth<sup>®</sup> with a direct connection to the MS-spectrometer *via* the mass flow controller.

### Ionic liquid synthesis

***n*-Bu<sub>4</sub>POAc.** The synthesis of *n*-Bu<sub>4</sub>POAc is adapted from ref. 47 and modified to our preparative demands. In a 100 ml round bottom flask 50 ml 40 wt% tetrabutylphosphonium hydroxide solution (72.4 mmol; *n*-Bu<sub>4</sub>POH) is mixed with 4.12 ml (72.4 mmol) of 99% acetic acid under vigorous stirring. After further stirring for 25 min the residual water is removed under reduced pressure at 60 °C. The resulting ionic liquid is further dried under reduced pressure for 72 h leaving a hygroscopic waxy solid behind. Yield 20.8 g (95%). <sup>1</sup>H-NMR (300 MHz, rt, CDCl<sub>3</sub>): δ (ppm) = 2.07–2.18 m (8H), 1.48–1.58 q (8H), 1.36–1.48 q (8H), 0.86–0.93 t (12H). <sup>31</sup>P-NMR (60 MHz, rt, CDCl<sub>3</sub>): δ (ppm) = 33.25.

**(*n*-Bu<sub>4</sub>P)<sub>2</sub>SO<sub>4</sub>.** Tetrabutylphosphonium sulphate was synthesized analogously with a 10% sulphuric acid solution (72.4 mmol). The resulting ionic liquid was a hygroscopic waxy solid. Yield: 27.8 g (99%) <sup>1</sup>H-NMR (300 MHz, rt, CDCl<sub>3</sub>): δ (ppm) = 2.06–2.18 q (8H), 1.47–1.59 q (8H), 1.36–1.48 q (8H), 0.86–0.93 t (12 H). <sup>31</sup>P-NMR (60 MHz, rt, CDCl<sub>3</sub>): δ (ppm) = 33.25.

All other ILs were synthesized according to literature known methods.<sup>7,9,42,70,71</sup>

### Nanoparticle synthesis

The Cu<sub>2</sub>O nanoparticles were synthesized in an oven-dried 25 ml crimp top vial equipped with a butyl-rubber septum and a glass stirring bar. 1 mmol (221 mg) basic CuCO<sub>3</sub> was suspended in 1 g IL and heated to 120 °C for 3 h while stirring at 500 rpm in a vial holder. The resulting precipitate was a brownish red dispersion of Cu<sub>2</sub>O nanoparticles in IL. The particles in IL could be easily dispersed in acetone, ethanol or isopropanol.

### Sample preparation for TEM analysis

A droplet of Cu<sub>2</sub>O-NPs embedded in IL was dispersed in acetone and a slight amount of this dispersion was placed in a holey carbon-coated copper grid. Particle size distributions were determined from the digital images obtained with a CCD camera. The NPs diameter was estimated from ensembles of 400 particles (800 counts) chosen in arbitrary areas of the enlarged micrographs. The diameters of the particles in the micrographs were measured using the software Sigma Scan Pro 5 and Lince Linear Intercept 2.4.2.

### Sample preparation for XRD analysis

The nanoparticle dispersion was dispersed in 10 ml acetone and centrifuged to yield a dark brown precipitate, which was filtered off and washed three times with acetone. The powder was dried under vacuum and prepared between two plastic disks before measurement.

### Procedure for protodecarboxylation reactions

The resulting nanoparticle dispersion was cooled to room-temperature (see Nanoparticle synthesis). 1 mmol 2-nitrobenzoic acid **1** (167 mg; 1 mmol) was then added to the dispersion and heated to 120 °C for 24 h. After cooling to room

temperature the reaction mixture was extracted with 3 × 10 ml Et<sub>2</sub>O. The organic phase was separated and the solvent removed under reduced pressure. The residue was analysed by <sup>1</sup>H-NMR (internal standard: hexamethyldisilane, 0.1 mmol, 20 μl) and compared with literature data. In the chemo-selectivity experiments 1 mmol of benzoic acids (**12**, **13**, **15–18**, **23**, **24**) was added to the mixture.

## Conclusions

We have shown a versatile and simple method to synthesize Cu<sub>2</sub>O nanoparticles in tetrabutylphosphonium acetate and sulphate resulting in small and uniformly sized nanocatalysts with an average diameter of 5.5 nm (±1.2 nm) and 8.0 nm (±2.7 nm), respectively. These incorporated nanoparticles are very potent in catalysing protodecarboxylation reactions of 2-nitrobenzoic acid **1** and derivatives with low catalyst loadings especially in recycling reactions. The IL–nanocat. system was compared to other IL–nanocat. systems with different polar and nonpolar ionic liquids as well as different copper-precursors, showing predominance concerning yield and recyclability. This catalytic phase, consisting of nanocatalysts in the ionic liquid, is superior for recycling experiments and can be recycled up to ten times, pointing out that this is the first nanoscale and the first recyclable catalyst proven to be active in decarboxylation reactions.

## Acknowledgements

We acknowledge the Ministerium für Innovation, Wissenschaft und Forschung NRW (MIWF-NRW) for financial support within the Energy Research Program for the Scientist Returnee Award (NRW-Rückkehrerprogramm) for Dr M. H. G. Prechtl. Furthermore, the Evonik<sup>®</sup> Foundation is acknowledged for a scholarship (M. T. Keßler) and the Robert-Lösch-Foundation for a project grant. Moreover, we are thankful to Dr L. Greiner and Dr S. Mariappan for their support at the Dechema Institute in performing the TEM analysis.

## Notes and references

- 1 A. Fukuoka and P. L. Dhepe, *Chem. Rec.*, 2009, **9**, 224–235.
- 2 J. Julis, M. Holscher and W. Leitner, *Green Chem.*, 2010, **12**, 1634–1639.
- 3 A. Behr, J. Eilting, K. Irawadi, J. Leschinski and F. Lindner, *Green Chem.*, 2008, **10**, 13–30.
- 4 D. Astruc, *Inorg. Chem.*, 2007, **46**, 1884–1894.
- 5 M. H. G. Prechtl, J. D. Scholten and J. Dupont, *Molecules*, 2010, **15**, 3441–3461.
- 6 A. G. Myers, D. Tanaka and M. R. Mannion, *J. Am. Chem. Soc.*, 2002, **124**, 11250–11251.
- 7 M. H. G. Prechtl, M. Scariot, J. D. Scholten, G. Machado, S. R. Teixeira and J. Dupont, *Inorg. Chem.*, 2008, **47**, 8995–9001.
- 8 M. H. G. Prechtl, J. D. Scholten and J. Dupont, *J. Mol. Catal. A: Chem.*, 2009, **313**, 74–78.

- 9 M. H. G. Precht, P. S. Campbell, J. D. Scholten, G. B. Fraser, G. Machado, C. C. Santini, J. Dupont and Y. Chauvin, *Nanoscale*, 2010, **2**, 2601–2606.
- 10 T. Gutel, J. Garcia-Anton, K. Pelzer, K. Philippot, C. C. Santini, Y. Chauvin, B. Chaudret and J. M. Basset, *J. Mater. Chem.*, 2007, **17**, 3290–3292.
- 11 T. Gutel, C. C. Santini, K. Philippot, A. Padua, K. Pelzer, B. Chaudret, Y. Chauvin and J. M. Basset, *J. Mater. Chem.*, 2009, **19**, 3624–3631.
- 12 P. S. Campbell, C. C. Santini, F. Bayard, Y. Chauvin, V. Colliere, A. Podgorsek, M. F. C. Gomes and J. Sa, *J. Catal.*, 2010, **275**, 99–107.
- 13 P. S. Campbell, C. C. Santini, D. Bouchu, B. Fenet, K. Philippot, B. Chaudret, A. A. H. Padua and Y. Chauvin, *Phys. Chem. Chem. Phys.*, 2010, **12**, 4217–4223.
- 14 G. Salas, A. Podgorsek, P. S. Campbell, C. C. Santini, A. A. H. Padua, M. F. C. Gomes, K. Philippot, B. Chaudret and M. Turmine, *Phys. Chem. Chem. Phys.*, 2011, **13**, 13527–13536.
- 15 G. Salas, C. C. Santini, K. Philippot, V. Colliere, B. Chaudret, B. Fenet and P. F. Fazzini, *Dalton Trans.*, 2011, **40**, 4660–4668.
- 16 C. W. Scheeren, G. Machado, S. R. Teixeira, J. Morais, J. B. Domingos and J. Dupont, *J. Phys. Chem. B*, 2006, **110**, 13011–13020.
- 17 G. S. Fonseca, A. P. Umpierre, P. F. P. Fichtner, S. R. Teixeira and J. Dupont, *Chem.–Eur. J.*, 2003, **9**, 3263–3269.
- 18 G. S. Fonseca, J. D. Scholten and J. Dupont, *Synlett*, 2004, 1525–1528.
- 19 J. Dupont, G. S. Fonseca, A. P. Umpierre, P. F. P. Fichtner and S. R. Teixeira, *J. Am. Chem. Soc.*, 2002, **124**, 4228–4229.
- 20 M. H. G. Precht, J. D. Scholten and J. Dupont, in *Ionic Liquids: Applications and Perspectives*, ed. A. Kokorin, InTech Vienna, 2011, pp. 393–414.
- 21 C. C. Cassol, A. P. Umpierre, G. Machado, S. I. Wolke and J. Dupont, *J. Am. Chem. Soc.*, 2005, **127**, 3298–3299.
- 22 C. S. Consorti, R. F. de Souza, J. Dupont and P. A. Z. Suarez, *Quim. Nova*, 2001, **24**, 830–837.
- 23 A. Balanta, C. Godard and C. Claver, *Chem. Soc. Rev.*, 2011, **40**, 4973–4985.
- 24 E. Raluy, I. Favier, A. M. Lopez-Vinasco, C. Pradel, E. Martin, D. Madec, E. Teuma and M. Gomez, *Phys. Chem. Chem. Phys.*, 2011, **13**, 13579–13584.
- 25 I. Favier, D. Madec, E. Teuma and M. Gomez, *Curr. Org. Chem.*, 2011, **15**, 3127–3174.
- 26 I. Favier, A. B. Castillo, C. Godard, S. Castillon, C. Claver, M. Gomez and E. Teuma, *Chem. Commun.*, 2011, **47**, 7869–7871.
- 27 L. Rodriguez-Perez, C. Pradel, P. Serp, M. Gomez and E. Teuma, *ChemCatChem*, 2011, **3**, 749–754.
- 28 D. Sanhes, E. Raluy, S. Retory, N. Saffon, E. Teuma and M. Gomez, *Dalton Trans.*, 2010, **39**, 9719–9726.
- 29 S. Jansat, J. Durand, I. Favier, F. Malbosc, C. Pradel, E. Teuma and M. Gomez, *ChemCatChem*, 2009, **1**, 244–246.
- 30 F. Fernandez, B. Cordero, J. Durand, G. Muller, F. Malbosc, Y. Kihn, E. Teuma and M. Gomez, *Dalton Trans.*, 2007, 5572–5581.
- 31 S. Jansat, M. Gomez, K. Philippot, G. Muller, E. Guiu, C. Claver, S. Castillon and B. Chaudret, *J. Am. Chem. Soc.*, 2004, **126**, 1592–1593.
- 32 M. Scariot, D. O. Silva, J. D. Scholten, G. Machado, S. R. Teixeira, M. A. Novak, G. Ebeling and J. Dupont, *Angew. Chem., Int. Ed.*, 2008, **47**, 9075–9078.
- 33 M. Mayer, A. Welther and A. Jacobi von Wangelin, *ChemCatChem*, 2011, **3**, 1567–1571.
- 34 J. D. Scholten, M. H. G. Precht and J. Dupont, in *Handbook of Green Chemistry*, ed. P. T. Anastas, Wiley Interscience, Weinheim, 2011, vol. 8, DOI: 10.1002/9783527628698.hgc9783527628085.
- 35 N. Yan, Y. A. Yuan, R. Dykeman, Y. A. Kou and P. J. Dyson, *Angew. Chem., Int. Ed.*, 2010, **49**, 5549–5553.
- 36 C. X. Xiao, Z. P. Cai, T. Wang, Y. Kou and N. Yan, *Angew. Chem., Int. Ed.*, 2008, **47**, 746–749.
- 37 D. Raut, K. Wankhede, V. Vaidya, S. Bhilare, N. Darwatkar, A. Deorukhkar, G. Trivedi and M. Salunkhe, *Catal. Commun.*, 2009, **10**, 1240–1243.
- 38 M. Swadzba-Kwasny, L. Chancelier, S. Ng, H. G. Manyar, C. Hardacre and P. Nockemann, *Dalton Trans.*, 2012, **41**, 219–227.
- 39 L. D. Pachon and G. Rothenberg, *Appl. Organomet. Chem.*, 2008, **22**, 288–299.
- 40 R. S. Schwab, D. Singh, E. E. Alberto, P. Piquini, O. E. D. Rodrigues and A. L. Braga, *Catal. Sci. Technol.*, 2011, **1**, 569–573.
- 41 V. Calo, A. Nacci, A. Monopoli and F. Montingelli, *J. Org. Chem.*, 2005, **70**, 6040–6044.
- 42 D. B. Zhao, Z. F. Fei, T. J. Geldbach, R. Scopelliti and P. J. Dyson, *J. Am. Chem. Soc.*, 2004, **126**, 15876–15882.
- 43 S. R. Dubbaka, D. B. Zhao, Z. F. Fei, C. M. R. Volla, P. J. Dyson and P. Vogel, *Synlett*, 2006, 3155–3157.
- 44 M. B. Thathagar, J. Beckers and G. Rothenberg, *Green Chem.*, 2004, **6**, 215–218.
- 45 V. Calo, A. Nacci, A. Monopoli, E. Ieva and N. Cioffi, *Org. Lett.*, 2005, **7**, 617–620.
- 46 J. H. Li, B. X. Tang, L. M. Tao, Y. X. Xie, Y. Liang and M. B. Zhang, *J. Org. Chem.*, 2006, **71**, 7488–7490.
- 47 C. T. Yang, Y. Fu, Y. B. Huang, J. Yi, Q. X. Guo and L. Liu, *Angew. Chem., Int. Ed.*, 2009, **48**, 7398–7401.
- 48 F. Nador, L. Fortunato, Y. Moglie, C. Vitale and G. Radivoy, *Synthesis*, 2009, 4027–4031.
- 49 J. Y. Kim, J. C. Park, H. Song and K. H. Park, *Bull. Korean Chem. Soc.*, 2010, **31**, 3509–3510.
- 50 T. J. Hu, X. R. Chen, J. Wang and J. Huang, *ChemCatChem*, 2011, **3**, 661–665.
- 51 P. P. Arquilliere, C. C. Santini, P. H. Haumesser and M. Aouine, *ECS Trans.*, 2011, **35**, 11–16.
- 52 F. Alonso and M. Yus, *ACS Catal.*, 2012, **2**, 1441–1451.
- 53 B. C. Ranu, R. Dey, T. Chatterjee and S. Ahammed, *ChemSusChem*, 2012, **5**, 22–44.
- 54 R. F. Heck and J. P. Nolley, *J. Org. Chem.*, 1972, **37**, 2320–2322.
- 55 H. J. Xu, Y. F. Liang, Z. Y. Cai, H. X. Qi, C. Y. Yang and Y. S. Feng, *J. Org. Chem.*, 2011, **76**, 2296–2300.

- 56 L. J. Goossen, R. T. Werner, N. Rodriguez, C. Linder and B. Melzer, *Adv. Synth. Catal.*, 2007, **349**, 2241–2246.
- 57 L. J. Goossen, F. Manjolinho, B. A. Khan and N. Rodriguez, *J. Org. Chem.*, 2009, **74**, 2620–2623.
- 58 R. A. Snow, C. R. Degenhardt and L. A. Paquette, *Tetrahedron Lett.*, 1976, 4447–4450.
- 59 J. Cornella, C. Sanchez, D. Banawa and I. Larrosa, *Chem. Commun.*, 2009, 7176–7178.
- 60 R. Venkatesan, M. H. G. Precht, J. D. Scholten, R. P. Pezzi, G. Machado and J. Dupont, *J. Mater. Chem.*, 2011, **21**, 3030–3036.
- 61 H. T. Liu, J. S. Owen and A. P. Alivisatos, *J. Am. Chem. Soc.*, 2007, **129**, 305–312.
- 62 H. Borchert, E. V. Shevehenko, A. Robert, I. Mekis, A. Kornowski, G. Grubel and H. Weller, *Langmuir*, 2005, **21**, 1931–1936.
- 63 Y. Zhong, D. H. Ping, X. Y. Song and F. X. Yin, *J. Alloys Compd.*, 2009, **476**, 113–117.
- 64 J. Dupont and J. D. Scholten, *Chem. Soc. Rev.*, 2010, **39**, 1780–1804.
- 65 B. K. Teo and N. J. A. Sloane, *Inorg. Chem.*, 1985, **24**, 4545–4558.
- 66 K. S. Weddle, J. D. Aiken and R. G. Finke, *J. Am. Chem. Soc.*, 1998, **120**, 5653–5666.
- 67 A. P. Umpierre, E. de Jesus and J. Dupont, *ChemCatChem*, 2011, **3**, 1413–1418.
- 68 L. Q. Xue, W. P. Su and Z. Y. Lin, *Dalton Trans.*, 2011, **40**, 11926–11936.
- 69 S. Seo, J. B. Taylor and M. F. Greaney, *Chem. Commun.*, 2012, **48**, 8270–8272.
- 70 C. C. Cassol, G. Ebeling, B. Ferrera and J. Dupont, *Adv. Synth. Catal.*, 2006, **348**, 243–248.
- 71 Y. G. Cui, I. Biondi, M. Chaubey, X. Yang, Z. F. Fei, R. Scopelliti, C. G. Hartinger, Y. D. Li, C. Chiappe and P. J. Dyson, *Phys. Chem. Chem. Phys.*, 2010, **12**, 1834–1841.